

# Developing Nanosuspension Loaded with Azelastine for Potential Nasal Drug Delivery: Determination of Proinflammatory Interleukin IL-4 mRNA Expression and Industrial Scale-Up Strategy

Yasir Mehmood,\* Hira Shahid, Muhammad Abbas, Umar Farooq, Sultan Alshehri, Prawez Alam, Faiyaz Shakeel, and Mohammed M. Ghoneim



Cite This: *ACS Omega* 2023, 8, 23812–23824

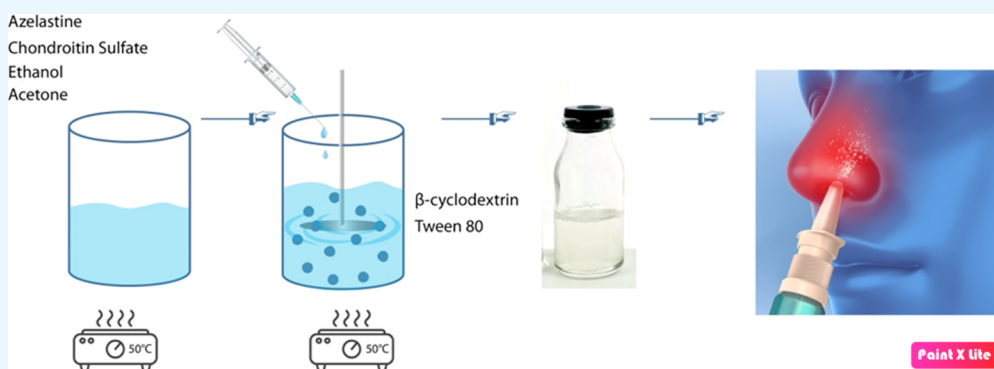


Read Online

ACCESS |

Metrics & More

Article Recommendations



**ABSTRACT:** In order to increase bioavailability and intranasal absorbance, the current work set out to create azelastine nasal spray based on nanosuspension. Chondroitin was utilized as a polymer to prepare azelastine nanosuspension through the precipitation procedure. A size of 500 nm and a polydispersity index of 0.276 with a negative potential ( $-20$  mV) were achieved. X-ray diffraction, scanning electron microscopy, Fourier transform infrared spectroscopy, thermal analysis including differential scanning calorimetry and thermogravimetric analysis, in vitro release, and diffusion studies were used to characterize the optimized nanosuspension. MTT assay was used to assess the viability of the cells, and hemolysis assay was used to assess the blood compatibility. Using RNA extraction and reverse transcription polymerase chain reaction, the levels of the anti-inflammatory cytokine IL-4, which is most closely related to cytokines in allergic rhinitis, were measured in mouse lungs. The drug dissolution and diffusion study indicated 2.0-fold increase compared to pure reference sample. Therefore, the azelastine nanosuspension could be suggested as a practical and simple nanosystem for intranasal delivery with improved permeability and bioavailability. The outcome obtained in this study indicated that azelastine nanosuspension has great potential to treat allergic rhinitis as intranasal treatment.

## 1. INTRODUCTION

A person's ability to operate normally and their quality of life can both be greatly impacted by chronic rhinitis, a common inflammatory condition that affects the paranasal sinuses and nasal cavity. It is typically identified by nasal discharge and congestion that lasts for at least 12 weeks.<sup>1,2</sup> The most frequent definition of rhinitis is a syndrome in which the patient has a number of chronic nasal symptoms, such as rhinorrhea, postnasal drip, nasal congestion, sneezing, and/or nasal pruritus.<sup>3</sup> Allergic and nonallergic rhinitis are the two basic categories into which rhinitis can be generally categorized.<sup>3</sup> For regulatory purposes, allergic rhinitis is categorized as either seasonal or perpetual in nature. An immunoglobulin E (IgE)-mediated response to seasonal allergens, such as outdoor mold spores or pollen from trees, grass, and weeds, results in seasonal allergic rhinitis. An IgE-mediated reaction to environmental allergens,

such as house dust mites, indoor fungi, and animal danders, which are typically present all year long, results in persistent allergic rhinitis.<sup>3</sup> The therapeutic approach for patients with rhinitis involves oral antihistamines and intranasal corticosteroids, which are the two most frequently utilized treatments for seasonal allergy rhinitis.<sup>4</sup> Steroids are frequently used to treat allergy rhinitis because of their strong anti-inflammatory effects.<sup>5,6</sup> Oral steroids are useful, but they can have a number

Received: April 1, 2023

Accepted: June 6, 2023

Published: June 21, 2023



of negative side effects.<sup>7,8</sup> A topical nasal spray called azelastine (AZN), a strong H1-antihistamine, is recommended for both seasonal allergic and nonallergic vasomotor rhinitis. It has been demonstrated to have a number of additional potentially significant properties in addition to its antihistaminic activities, including effects on cytokines, adhesion molecules, and inflammatory cells. This medication has antiallergic properties that include suppressing IgE antibody synthesis, antigen–antibody responses, releasing mediators, and antagonistic interactions among mediators. According to one study, AZN inhibited the cytokines interleukin-2 (IL-2), IL-3, and IL-4 in cultured cells.<sup>9</sup> Patients who have not responded well to loratadine and fexofenadine may benefit from azelastine nasal spray, which has been found to be much more effective than cetirizine and levocabastine in treating seasonal allergic rhinitis. AZN continues to play a significant role in the treatment of chronic rhinitis due to its distinct pharmacologic characteristics and clinical profile.<sup>3</sup> For more than 10 years, it has been utilized in clinical practice for rhinitis, and a sizable body of literature has shown its therapeutic characteristics for such illnesses. Lee and Corren conducted a thorough evaluation to see whether AZN nasal sprays were useful for treating rhinitis. AZN nasal spray significantly reduced rhinitis symptoms in severe acute respiratory syndrome patients who continued to experience them after receiving fexofenadine treatment when compared to oral antihistamines.<sup>3</sup>

The danger of systemic absorption is relatively low for the AZN medication, which is highly lipophilic and has poor water solubility (9.2  $\mu\text{g}/\text{mL}$ ). Additionally, AZN is sparingly soluble in methanol and propylene glycol and only marginally soluble in ethanol, octanol, and glycerine (log  $P$  is 2.3).<sup>10</sup> AZN has 40% systemic bioavailability (BA) after intranasal delivery, reaching peak plasma concentration ( $C_{\text{max}}$ ) after 2–3 h. One of the most significant issues with drug research is the inability of some pharmaceuticals to dissolve in water.<sup>11–15</sup> For insoluble drugs, excipients such as surfactants, cosolvents, micellar solutions, complexing agents, and lipid formulations are required to increase their solubility.<sup>16–19</sup> Unfortunately, the need for more materials to create weakly water-soluble compounds may increase the risk of negative outcomes. To increase the solubility and BA of medications that are poorly water-soluble, a number of strategies have been developed, including solid dispersion, complexation, lipid-based systems, micronization, nanonization, and cocrystals.<sup>18–20</sup> Nanotechnology-based medication delivery can get around some anatomical, physiological, pharmacological, and clinical problems with traditional dose forms in all of these technologies.<sup>21</sup> A few examples of the important therapeutic agents that can be given to several biological systems by nanoparticles (NPs), submicrometer particulate dispersions, or solid particles include nucleic acids, peptides, and tiny hydrophobic and hydrophilic molecules. Improved medication solubility and stability, higher BA at the site of application, and extended duration of action by regulating the release rate are some possible benefits of NPs.<sup>22</sup> Over the years, numerous varieties of nanotherapeutics have been developed and assessed (liposomes, polymers, and micelles as carrier materials).<sup>23</sup> Copolymers are a type of carrier material. Chondroitin polymer has several uses because of its excellent biocompatibility, which makes it a biomaterial and biodegradable. The characteristics of molecular mass and a wide variety of parameters can be used to adjust the biodegradation rate. The body quickly breaks down the hydrolyzed monomers through the Krebs cycle and excretes them as carbon dioxide and water.

Chondroitin is a bioactive polymer that has a wide range of uses because of its valuable qualities, which include antibacterial activity, nontoxicity, and adaptability.<sup>24</sup> The current study aimed to create a nasal spray of AZN based on nanosuspensions for enhanced BA by avoiding hepatic first-pass metabolism and patient compliance. The present study's objective was to develop and assess AZN nanosuspension formulation employing the organic phase-containing drug and polymer.

## 2. RESULTS AND DISCUSSION

Topical antihistamines are the first line of medicinal defense against the chronic inflammatory disease known as allergic rhinitis. A limited therapeutic response occurs due to the topical antihistamine's ineffective delivery to the nose and sinuses. When administering medications locally, using nanosuspension may help to improve treatment success by reducing systemic side effects, increasing contact duration, elevating local drug concentrations, and ensuring consistent distribution to target regions. A modified precipitation technique was used to make AZN nanosuspension. The formulation for the nasal spray was altered to include AZN nanosuspension in order to increase solubility, and stability was further explored (not added in the article). Table 1 shows the different ingredient concentrations in

**Table 1. Optimized Formulation of AZN Nanosuspension**

sr. #	material name	quantity of material used	percentage (%) of material
1.	azelastine	200 mg	0.66
2.	chondroitin	200 mg	0.66
3.	ethanol	10 mL	26.0
4.	tween-80	1.0 mL	3.53
5.	$\beta$ -cyclodextrin	1.00 g	3.30
6.	water	20 mL	65.80
total		30.3 g	99.95

mg and percentages. The results showed an entrapment efficiency and drug loading of  $67.9 \pm 5.1$  and  $11 \pm 0.6\%$ , respectively. A total of 30.3 g was prepared on a lab scale, which was converted into a pilot scale with a 100 kg batch size.

**2.1. Particle Size, Polydispersity Index, and Zeta Potential.** Dynamic light scattering (DLS) was used to determine and describe the AZN nanosuspension size, size distribution, and charge. Size distribution diagram of AZN nanosuspension generated in water is shown in Figure 1. The DLS results revealed that the nanosuspension had a hydrodynamic diameter of 500 nm and a polydispersity index (PDI) of  $0.276 \pm 0.08$ . A Malvern Zetasizer ZS200 was used to measure the zeta potential of the nanosuspension. The average value of AZN nanosuspension zeta potentials is about  $-20$  mV, and this is sufficient to fully stabilize the system.

**2.2. Fourier Transform Infrared Analysis.** As shown in Figure 2, the synthesized AZN nanosuspensions were examined using Fourier transform infrared (FTIR) spectroscopy in the spectrum region of  $800\text{--}4000$   $\text{cm}^{-1}$  for identification and characterization of the functional groups present. Pure AZN shows the peak at  $1631.17$   $\text{cm}^{-1}$  corresponding to the amide group in the drug. Most frequent peaks are seen from  $1000$  to  $1700$   $\text{cm}^{-1}$ , but more distinct peaks can be observed at  $1570$  and  $1690$   $\text{cm}^{-1}$ , which are due to N=N stretching.<sup>25</sup> Several distinguishing bands were seen when the FTIR spectra of native chondroitin were analyzed. O–H and N–H bond stretching vibrations are represented by a wideband at  $3400$   $\text{cm}^{-1}$ . It was

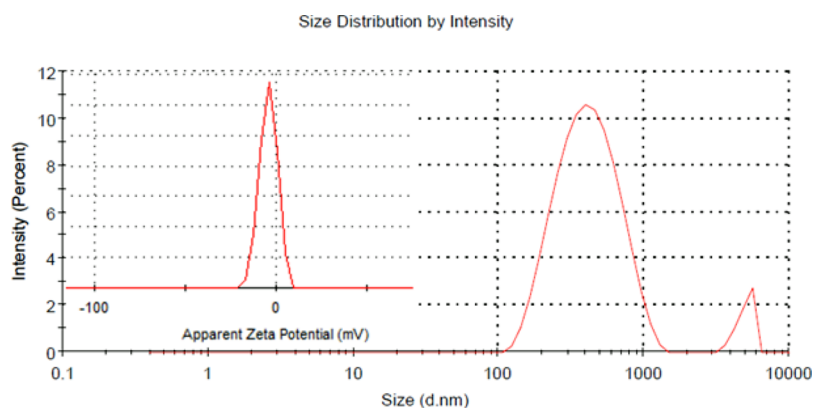


Figure 1. Size distributions and charge of AZN nanosuspension.

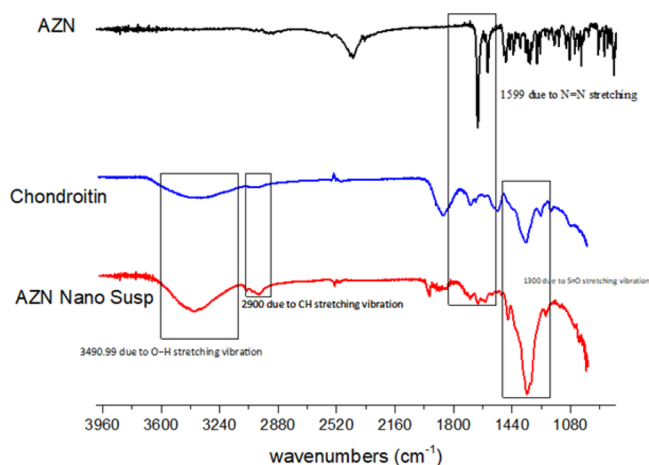


Figure 2. FTIR analysis of AZN, chondroitin, and AZN nanosuspension.

also observed that the stretching vibrations of N–H bonds overlap those of O–H bonds in this instance. The peak at  $2900\text{ cm}^{-1}$  is caused by the stretching vibrations of the C–H bonds in the  $-\text{CH}_2$  and  $-\text{CH}_3$  groups of aliphatic chains, both symmetrically and asymmetrically. The characteristic peak of chondroitin sulfate at  $1225\text{ cm}^{-1}$  corresponds to the stretching vibrations of S=O bonds. The distinctive peaks of AZN, including those at  $1334\text{ cm}^{-1}$  (C–N vibration),  $1671\text{ cm}^{-1}$  (C=N and C=C stretching), and  $1599\text{ cm}^{-1}$  (N=N stretching), were noticeably obscured in the AZN nanosuspension, as shown in the spectra (Figure 3). The peak intensities of C–H and O–H both changed slightly, going from  $2900$  to  $3000\text{ cm}^{-1}$  and  $3490.99\text{ cm}^{-1}$ , respectively. The characteristic peaks of chondroitin sulfate at  $1215$ ,  $3340$ , and  $2809.0\text{ cm}^{-1}$  were also found in AZN nanosuspension which were slightly displaced but within the range. It can be concluded that there was minimal interaction between AZT and chondroitin polymer, as evidenced by the change in peak intensity, which was a sign of chemical and physical changes occurring during the nanosuspension formation process. This interaction resulted in high entrapment efficiency of AZN into the polymer.

**2.3. Thermal Analysis.** Thermal analysis was used to evaluate AZN, chondroitin, and AZN nanosuspension. The response of AZN, chondroitin, and AZN nanosuspension against temperature is shown in Figure 3. Both characteristics differential scanning calorimetry (DSC) and thermal gravimetric

analysis (TGA) were determined with this apparatus. Figure 3 displays the findings of the DSC analysis of AZN, chondroitin, and AZN nanosuspension. As shown in Figure 3, the DSC curve of AZN exhibits an exothermic peak at  $60\text{ }^\circ\text{C}$ , which was due to partial loss of residual humidity. An exothermic peak is seen at  $240\text{ }^\circ\text{C}$ , which is the glass transition temperature ( $T_g$ ). The complicated thermal events occurring at about  $240\text{ }^\circ\text{C}$  show that AZN significantly degrades during melting. About the weight loss of AZN, it started from  $50$  to  $100\text{ }^\circ\text{C}$ , and the total weight loss was observed to be  $40\%$  in TGA (Figure 3), which was continued and at  $300\text{ }^\circ\text{C}$ ,  $90\%$  of drug was decomposed. A totally amorphous version of the polymer known as chondroitin exists at a  $T_g$  of roughly  $110\text{ }^\circ\text{C}$ . At a temperature of  $230\text{ }^\circ\text{C}$ , the transition peak in chondroitin was seen due to degradation. There was also a weight loss ( $30\%$ ) which was observed by TGA at  $60\text{ }^\circ\text{C}$ , and the total weight loss of chondroitin at  $300\text{ }^\circ\text{C}$  was about  $50\%$ . Due to dehydration and the removal of volatile components, the DSC curve of AZN nanosuspension displays an endothermic peak at  $60\text{ }^\circ\text{C}$ , which matches its intrinsic melting points.  $T_g$  is responsible for an exothermic peak that was seen at a temperature of about  $110\text{ }^\circ\text{C}$ . One more endothermic peak was observed at  $240\text{ }^\circ\text{C}$ , and the same peak was observed in AZN thermal analysis which indicates successful entrapment of AZN into the chondroitin polymer to form NPs. In this formulation, TGA showed a low weight loss of  $35\%$  at  $75\text{ }^\circ\text{C}$  and  $70\%$  till  $300\text{ }^\circ\text{C}$  which indicated that the formulation has low weight loss over  $300\text{ }^\circ\text{C}$  than the AZN pure form. In this case, the AZN weight loss shifts from  $90$  to  $70\%$  which indicated that AZN within chondroitin in the nano form is much stable.

**2.4. Morphology Analysis.** Following an electron microscopy scan of the particles, it was discovered that the AZN nanosuspension was spherical in shape. Scanning electron microscopy (SEM) micrographs of pure AZN (Figure 4) and an optimized nanosuspension formulation clearly demonstrated significant differences. Phase evaporation during particle hardening may be the cause of the AZN nanosuspension's disorderly form. This AZN nanosuspension is an essential feature of the delivery system due to the controlled release properties of the drug particles that are entrapped in it.<sup>26</sup> Figure 4B,C shows the SEM view of AZN nanosuspension, and the view showed well-dispersed particles. The result showed a successful nanosuspension with nonordered shape of particles. Figure 4A, which shows big crystal particles, also revealed API crystalline particles.

**2.5. PXRD Analysis.** The internal structure of the AZN pure drug crystal, chondroitin, and AZN nanosuspension was identified using powder X-ray diffraction (PXRD) analysis.

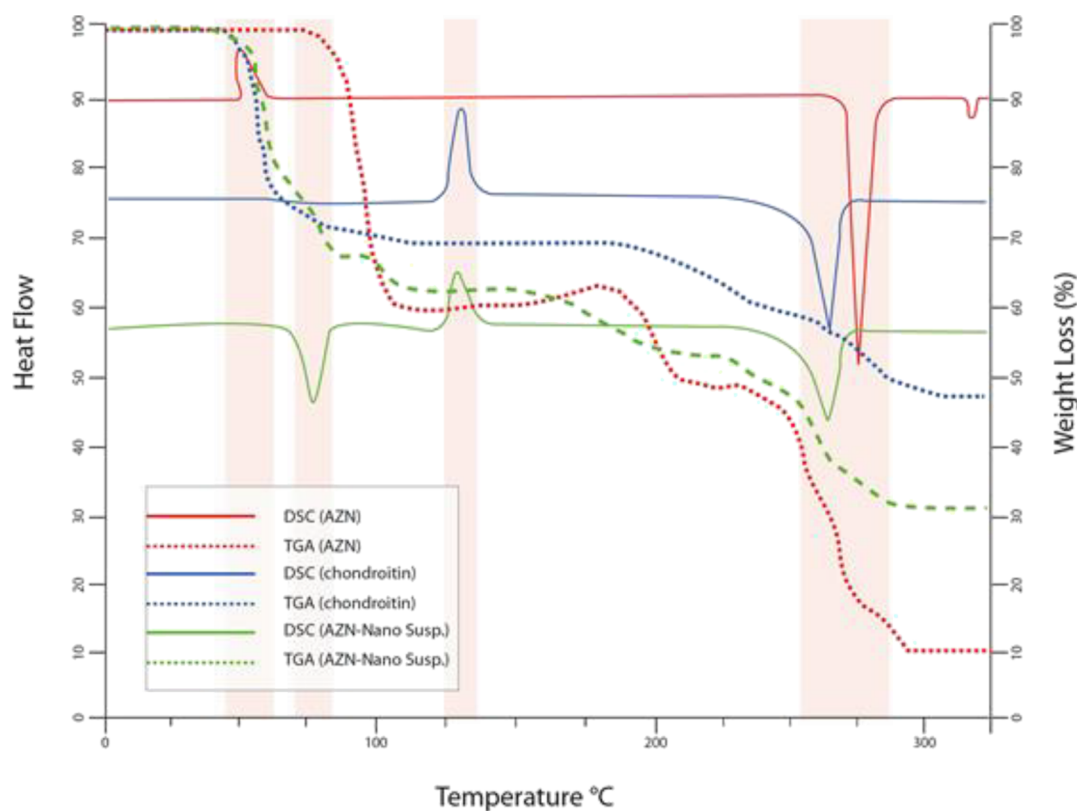


**Figure 3.** Thermal analysis (DSC and TGA) of AZN, chondroitin, and AZN nanosuspension.

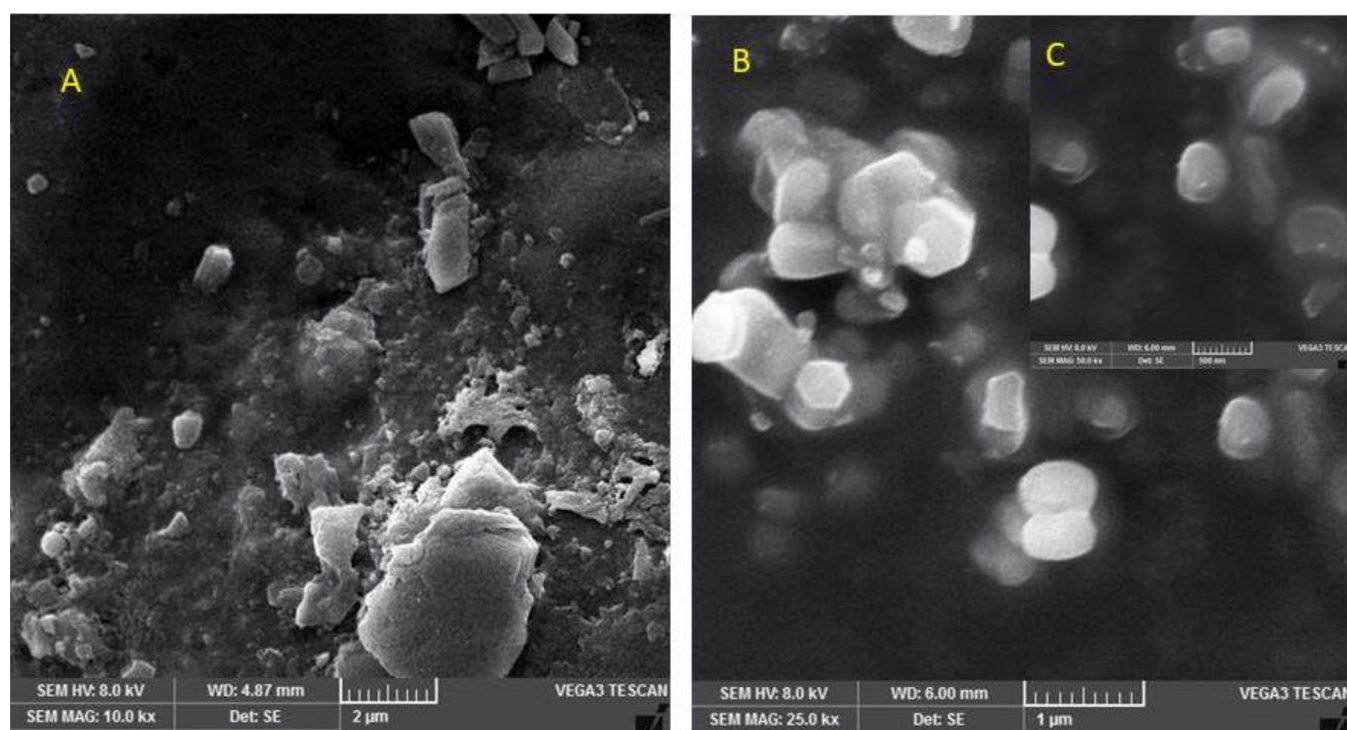


**Figure 4.** SEM images of AZN pure drug and AZN nanosuspension.

How much of these changes take place depends on the chemical composition and physical toughness of the active substance. [Figure 5](#) shows the PXRD patterns for AZN, chondroitin, and AZN nanosuspension. Sharp peaks with crystalline shapes are seen in AZN XRD. Polymorphic PXRD patterns with prominent

peaks were seen at 2-theta values of 90, 57, 54, 45, 90, 86, 41, 51, and 46°. However, due to expanded pore confinement with the polymer matrix, no obvious peaks were found in the AZN nanosuspension to corroborate the shift of AZN into the amorphous form. Only few peaks were seen at 2-theta of 57, 46,

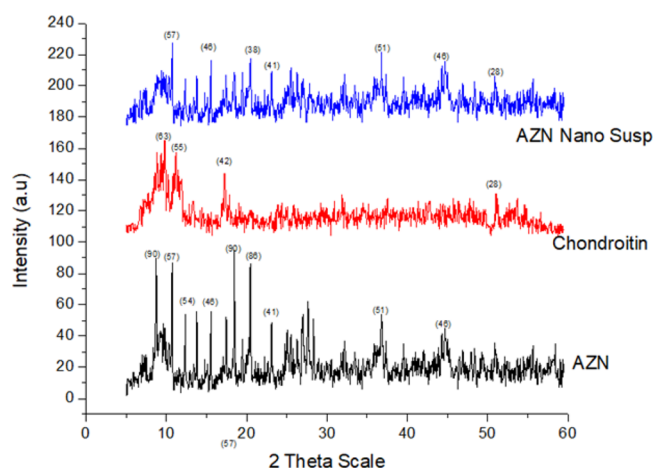


Figure 5. PXRD patterns of AZN pure drug and AZN nanosuspension.

38, 41, 51, and 46° with very low intensity which show AZN presence within the polymeric system in the amorphous form. Reflection peaks of AZN were still evident, showing that the crystalline form of AZN partly kept in the AZN nanosuspension; the AZN and the nanosuspension profiles were highly comparable.

**2.6. In Vitro Release Study.** AZN pure medication and AZN nanosuspension was checked for its dissolution study in two buffers up to 60 min. Release profile from both types is shown in Figure 6. AZN nanosuspension release profile

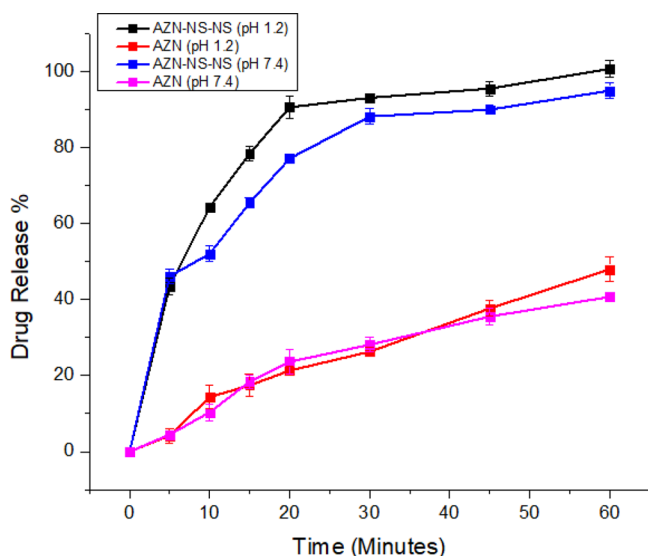


Figure 6. In vitro release profile of pure AZN and formulation studied at acidic buffer pH (1.2) and phosphate buffer (pH 7.4) according to the dialysis bag membrane method (mean  $\pm$  SD,  $n = 3$ ).

displayed immediate release pattern in the first step and sustained type in the second step that was biphasic in nature (Figure 6). The mean particle size of the AZN nanosuspension samples employed in this study was 500 nm which is helpful to increase the dissolution of the AZN nanosuspension in both media, and its rapid dissolution results in immediate release in the first step. Since the release of pure drugs is relatively slow and remain insoluble up to 60 min, it displayed a nearly identical pattern of low solubility in both media. AZN nanosuspension showed a rapid drug release pattern in the first 10 min and then a

continuous drug release pattern and 100 and 97% dissolved within 60 min in both buffers and pH. The initial rate of dissolution was inversely proportional to the size of the nanosuspension particles (Figure 6), which supported the method's ability to distinguish between different materials.

**2.7. Hemolysis Investigations.** Through hemolytic studies, the compatibility of the AZN nanosuspension with blood was examined. The hemolysis assay was used to evaluate the cytotoxic effect of NPs on RBCs because the nasal cavity membrane is sensitive. To determine 50% lysis of RBCs (TC<sub>50</sub>) of AZN nanosuspension, the RBCs were exposed to each AZN nanosuspension sample in a range of concentrations 100, 150, and 200  $\mu\text{g}/\text{mL}$ . These concentrations were used because one-time actuator dose of AZN was in micrograms. Hemolytic analyses revealed that the AZN nanosuspension did not cause any hemolysis after administration at concentrations of 100, 150, and 200  $\mu\text{g}/\text{mL}$ . However, negligible hemolysis was noted even at a high concentration of 200  $\mu\text{g}/\text{mL}$  (13.25%), but it was also less than 50%, and blood cells demonstrated well-considerable tolerance to the complex ( $R^2 = 0.9953$ ). The current study's findings showed (Figure 7) that hemolysis investigation is a tool

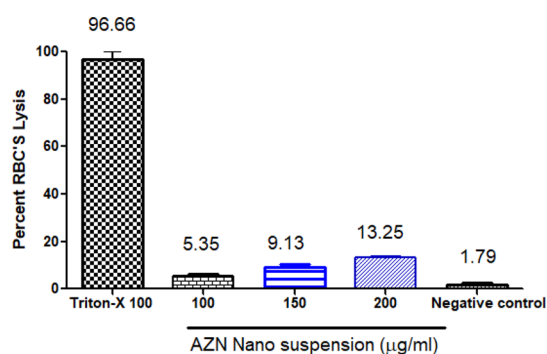
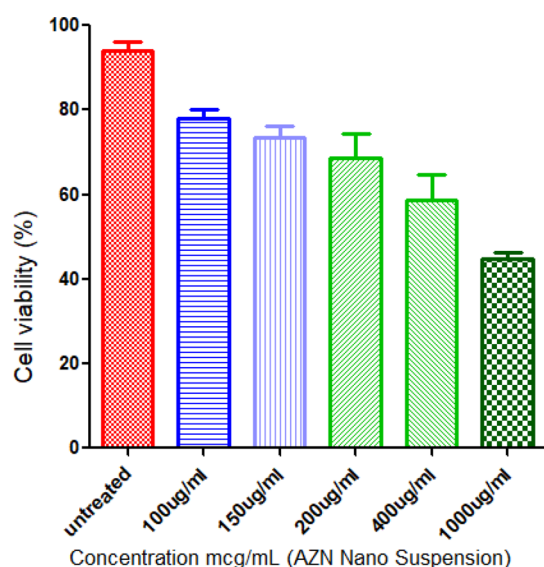


Figure 7. Compatibility of AZN nanosuspension with blood (mean  $\pm$  SD,  $n = 3$ ).

to demonstrate the RBC and sample compatibility after incubation, and it can be further investigated or confirmed by the MTT assay which we have performed in Section 2.8.

**2.8. In Vitro Cell Viability Testing.** HepG2 cells over five different concentrations along with untreated cells were used to determine the cell viability. This investigation was performed to determine the cell and sample compatibility. Different concentrations were used which were in micrograms because AZN clinical dose was also in microgram as per literature review. The highest dose (1000  $\mu\text{g}$ ) used in this work was chosen to model doses often used for in vivo biodistribution and therapeutic experiments. In previous experiments (hemolysis investigation), we have used three concentrations, and in this experiment, we used five different concentrations to find the IC<sub>50</sub> value. The total cell number was normalized in the untreated group, and there was no significant toxicity found in each concentration of AZN nanosuspension (Figure 8). The concentration of AZN nanosuspension in water (untreated cells) is nearly nontoxic and biocompatible. Percentage cell viability was checked at 100, 150, 200, 400, and 1000  $\mu\text{g}/\text{mL}$  of AZN nanosuspension and was found to be  $78.06 \pm 0.36$ ,  $73.36 \pm 0.08$ ,  $68.71 \pm 0.09$ ,  $58.71 \pm 0.10$ , and  $44.76 \pm 0.07$   $\mu\text{g}/\text{mL}$ , respectively, demonstrating the dose-dependent pattern of cytotoxicity which will be considered as the nonsignificant toxicity of AZN nanosuspension. The result of IC<sub>50</sub> of the AZN



**Figure 8.** Percentage viability checked at 100, 150, 200, 400, and 1000  $\mu\text{g}/\text{mL}$  of AZN nanosuspension (mean  $\pm$  SD,  $n = 3$ ).

nanosuspension after 24 h of exposure toward HepG2 cells was 893.35  $\mu\text{g}/\text{mL}$  indicating relatively nontoxic nature.

**2.9. Effect of AZN Nanosuspension on the IL-4 mRNA Expression Level.** A total of four groups were used in this study and were divided into one control group and three diseased groups. Diseased groups were sensitized with ovalbumin (OVA) solution for 14 days, and the controlled group (I) was sensitized with phosphate-buffered saline (PBS). Each day, OVA solution was given to all three diseased groups. After 14 days, two diseased groups (III and IV) were treated with the AZN nanosuspension and pure drug suspension through the intranasal route one time a day according to standard dose (137  $\mu\text{g}/\text{kg}/\text{day}$ ) till 28 days. One diseased group (II) was continued to be sensitized with OVA solution till 28 days. After completion of 28 days, the mice were sacrificed and checked. The information showed that the diseased group's interleukin 4 (IL-4) mRNA expression levels were higher than those of the control group. When we compared the diseased group with treated groups (AZN nanosuspension and pure drug suspension), we found significantly decreased levels of IL-4 mRNA expression in the treated groups. The results show that group III and group IV had significantly lower mRNA levels of IL-4 than group II (diseased) ( $6.781 \pm 0.117$  vs  $5.386 \pm 0.189$ ). The group which was treated with AZN had the lowest level of mRNA IL-4, which was very near to the control group due to its rapid absorption in mouse blood and lungs. Results indicated that the AZN nanosuspension has potential against allergic rhinitis when compared to pure drug (Figure 9).

**2.10. Significant Reduction of TLC and DLC in Blood by AZN Nanosuspension.** Blood analysis was done for four groups of mice [control, diseased, AZN nanosuspension, and pure drug (137  $\mu\text{g}$  concentration was used for pure drug and nanosuspension)]. Control group of mice was treated with simple water phosphate buffer till 28 days. Rest of three groups were engaged with OVA challenge. After 14 days, two groups started treatment with sample drugs and diseased groups was engaged with OVA till 28 days. Total leucocyte count (TLC) and differential leucocyte count (DLC) were measured in all groups. After blood analysis of all groups, the reports show that the total leucocytes, lymphocytes, neutrophils, monocytes, and eosino-

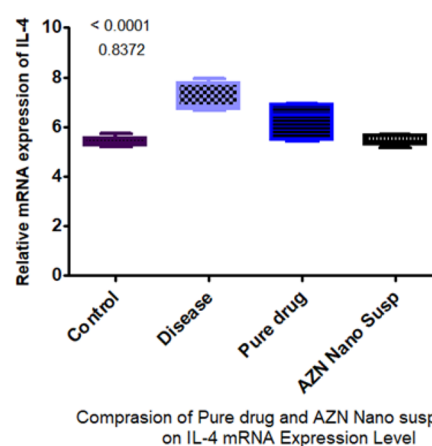


**Figure 9.** Effect of AZN pure drug and AZN nanosuspension on IL-4 mRNA expression level (mean  $\pm$  SD,  $n = 6$ ).

phil counts of the diseased group were considerably greater than those of the control group. In comparison to the control group of mice, the sick group's blood had significantly more leucocytes, lymphocytes, neutrophils, monocytes and eosinophils (all  $p < 0.001$ ). Treatment with AZN nanosuspension led to a significant drop (all  $p < 0.001$ ) in DLC as compared to the group receiving pure drug (Table 2). Results show that the AZN nanosuspension also significantly decreases or overcomes the TLC and DLC parameters in the diseased mouse.

**2.11. Nasal Ciliotoxicity Study.** To assess any potential negative effects of AZN nanosuspension, studies on nasal ciliotoxicity were conducted. A fixed concentration of 137  $\mu\text{g}$  was applied to determine the ciliotoxicity because this is the clinical dose per actuator. Contrary to the positive control (ethanol), this significantly damaged the nasal mucosa and caused loss of nasal cilia (Figure 10B). In the group which was treated with PBS, the nasal membrane remained unharmed (negative control) and did not exhibit any nasociliary damage (Figure 10A). However, in AZN nanosuspension, there was no evidence of nasal mucosa injury (Figure 10C), demonstrating the safety of the formulation's AZN nanosuspension.

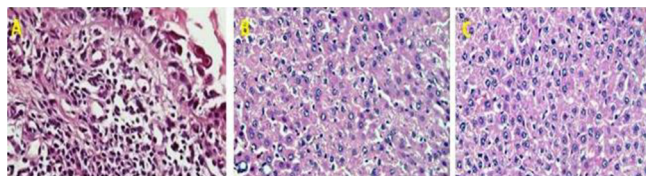
**2.12. Post Preparation Test.** **2.12.1. Microbiological Studies.** Once the AZN nanosuspension has been converted into nasal spray formulation for patients use, it must meet all USP 43 criteria along with microbial specifications.<sup>27</sup> Total aerobic microbial count (TAMC), total yeast and mold count (TYMC), and staphylococcus and pseudomonas were checked after formulation scale up. We have used gold standard method to observe colony forming units (CFUs) on plates. Sabouraud dextrose agar and nutrient agar were used to prepare the plates. Plates were prepared as previously mentioned in the literature.<sup>28</sup> Plates were incubated in Memmert incubators for 72 h for TAMC and 7 days for TYMC at different temperatures. Results are shown in Table 3.

**2.12.2. Physical Characterization.** AZN nanosuspension nasal spray (AZN-NS-NS) formulation was created in liquid form for nasal spray uses. According to USP, the pH of the formulation for the AZN-NS-NS was  $6.1 \pm 0.5$ , which is suitable for nasal products. At 25  $^{\circ}\text{C}$ , the formulation's viscosity was  $79 \pm 0.8$  cps which is also suitable for intranasal use. Homogeneity and clarity were found satisfactory for both products (Table 4).

**2.12.3. In Vitro Permeability.** The current study's main objective was to assess the AZN nanosuspension permeability over the silica membrane in vitro (pH 6.8). According to Figure

**Table 2. TLC and DLC in Blood in all Groups (Mean  $\pm$  SD,  $n = 6$ )**

parameters (blood)	group I (control)	group II (disease)	group III AZN nano suspension 137 $\mu$ g	group IV pure dug 137 $\mu$ g
TLC 1000/ul	6.2 $\pm$ 1.53	11.28 $\pm$ 1.73	8.04 $\pm$ 1.29	6.92 $\pm$ 0.52
lymphocytes %	4.9 $\pm$ 0.56	5.9 $\pm$ 0.1	4.2 $\pm$ 0.17	3.5 $\pm$ 0.14
neutrophils %	1.16 $\pm$ 0.08	2.5 $\pm$ 0.56	1.35 $\pm$ 0.12	1.7 $\pm$ 0.35
eosinophils %	0.18 $\pm$ 0.04	0.27 $\pm$ 0.09	0.19 $\pm$ 0.09	0.43 $\pm$ 0.012
monocytes %	0.24 $\pm$ 0.11	0.97 $\pm$ 0.01	0.31 $\pm$ 0.11	0.79 $\pm$ 0.03
basophils %	0.05 $\pm$ 0.009	0.12 $\pm$ 0.002	0.03 $\pm$ 0.009	0.12 $\pm$ 0.031

**Figure 10.** Histopathology of sheep nasal mucosa. Nasal mucosa (A) treated with PBS, (B) treated with ethanol, and (C) treated with AZN nanosuspension.

11, the results showed that the AZN nanosuspension diffused by 2 folds at pH 6.8 as compared with pure drug. The smaller particle sizes obtained through precipitation method contributed to this improvement.

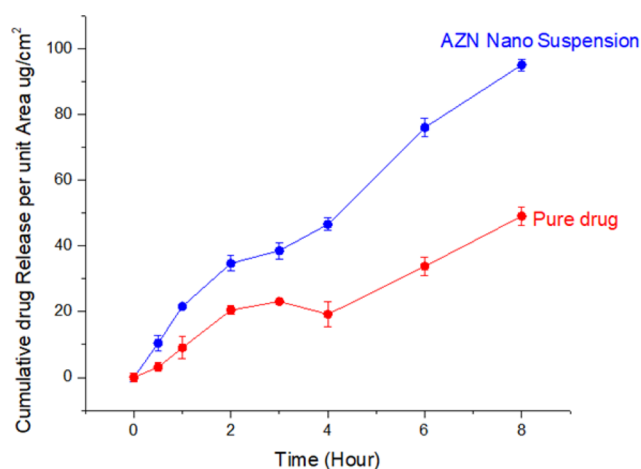
**2.12.4. Nanosuspension Dosage Forms: Process Variable and Scale Up.** The scale-up procedure is carried out after the product and its process leave the development laboratory but before it is approved for the pilot program. After the pilot batch which must be equal to commercial batch, the product can be marketed. Following accelerated, elevated temperature testing which confirms that the (1 $\times$ ) laboratory batch is both physically and chemically robust, the scale-up procedure is the fabrication of the (10 $\times$ ) laboratory batch. Once the pilot batch is manufactured in well means, three commercial batches are involve for process validation (i.e., product and process qualification studies). For our product, we have a 100 kg batch which was manufactured using large scale equipment. Critical process parameters and critical quality attributes (CPPs and CQAs) were highlighted during the lab scale batch, and then these parameters were observed and tested as mentioned in Figure 12. There are several critical parameters mentioned in Table 5 with its occurrence scale like high, median, and low. Results showed that all critical parameters were well controlled, and the results were within specifications according to USP 43 pharmacopeia. Different instruments were used to check the assay and content uniformity, viscosity, pH, and particle size. Process capability index ( $C_{pk}$ ) is a statistical tool used to assess the capacity of a process to deliver results within the confines of customer specifications. Process capability index has been shown in Table 6.  $C_{pk}$  has been the index that is most frequently employed in practice. In this paper, we have also calculated the

**Table 3. Microbial Limit Test Results According to USP 43**

description	results (cfu/mL)			
	batch # 001	batch # 002	batch # 003	limits
total aerobic microbial count (TAMC)	<10 cfu/mL	<10 cfu/mL	<10 cfu/mL	200 cfu/mL
total combined yeasts & molds count (TYMC)	<10 cfu/mL	<10 cfu/mL	<10 cfu/mL	20 cfu/mL
Tests for Absence of Specified Microorganisms				
<i>Staphylococcus aureus</i>	absent/mL	absent/mL	absent/mL	should be absent/mL
<i>Pseudomonas aeruginosa</i>	absent/mL	absent/mL	absent/mL	should be absent/mL

**Table 4. Compression of Prepared Nasal Spray and Commercial Nasal Spray Parameters (Mean  $\pm$  SD,  $n = 3$ )**

formulation	clarity	pH	homogeneity	viscosity cps
AZN nanosuspension nasal spray	clear	6.1 $\pm$ 0.5	good	79 $\pm$ 0.8
commercial product (azocin)	clear	6.8 $\pm$ 0.6	good	69 $\pm$ 1.6

**Figure 11.** AZN release from AZN nanosuspension through silicon membrane compared with pure drug (mean  $\pm$  SD,  $n = 3$ ).

$C_{pk}$  values of three batches regarding their CQAs which indicated that the process is capable.

### 3. DISCUSSION

An inflammation of the nose and paranasal sinuses, known as chronic rhinosinusitis, is characterized by two or more symptoms, at least one of which must be nasal obstruction, congestion, blockage, or discharge.<sup>29</sup> Drug delivery based on nanotechnology can get around several anatomical, physiological, chemical, and therapeutic problems with traditional dosage forms. Nanoparticles (NPs) are submicrometer particulate dispersions or solid particles that can transport a range of therapeutic agents to various biological systems, including nucleic acids, peptides, and small hydrophobic and



Figure 12. CPCs and CQAs for large-scale batch.

Table 5. Scale Up of Optimized Formulation

sr. #	material name	quantity of material used (kg)	percentage (%) of material
1.	azelastine	0.66	0.66
2.	chondroitin	0.66	0.66
3.	ethanol	26.04	26.04
4.	tween-80	3.53	3.53
5.	$\beta$ -cyclodextrin	3.30	3.30
6.	water	65.80	65.80
	total	99.99	99.99

Table 6. Capability Index of CQAs

sr. #	critical parameter	$C_p/C_{pk}$ value
1	viscosity (0.4–0.5 Pa S)	1.48
2	density (0.9–1.1 g/cm <sup>3</sup> )	5.34
3	content uniformity (85–115%)	1.76
4	assay (80–120%)	1.97
5	pH	1.9
6	particle size distribution	1.7
7	MLT	1.8

hydrophilic compounds.<sup>30</sup> Improved medication solubility and stability, higher BA at the targeted site, and prolonged duration of action by regulating the release rate are some possible benefits of NPs.<sup>31</sup> The creation of the AZN nasal formulation involved straightforward methods of preparation. A potential platform for the nasal distribution of AZN was shown by the combination of nanosuspension and the straightforward addition of a NEOCEL C91 solution. The sonicated approach, along with polymers, changes AZN crystallinity into amorphous through nanosizing. As a result, the compositions' long-term temporal stability might be enhanced. Additionally, it has a higher diffusion and permeability coefficient than neat drugs. The results of the in vivo investigations provided evidence that the nasal delivery of AZN was safe. Scaling up a nanomedicine product involves a number of steps before it reaches the market. For instance, the type of material and its general acceptance of safety (GRAS) status and toxicological characteristics are linked to the nanoparticle size and shape. After the pilot batch, which must be equal to the commercial batch, the product can be marketed.

#### 4. CONCLUSIONS

According to the results of this investigation, AZN nanosuspension is a highly effective formulation for the prospective treatment of allergic rhinitis. To the best of our knowledge, this is the first account of a preparation for nasal drug delivery based

on nanoprecipitation containing AZN. The successfully prepared AZN nanosuspension had appropriate physicochemical properties, high drug loading content, and effective drug encapsulation. The preparation process of AZN nanosuspension is quite facile. XRD pattern indicates the formation of an amorphous structure of AZN, and the average particle size is found to be 500 nm. The AZN nanosuspension also shows permissible limit of hemolysis activity at its lower concentration, and hence, this can be considered as biocompatible. Cytotoxicity (MTT assay) of AZN nanosuspension was very low in all nasal concentrations (treated and untreated). We think that the AZN nanosuspension for intranasal delivery will be a promising strategy for enhancing local treatment of allergic rhinitis, and therefore, their potential for nasal administration applications calls for additional in vitro and in vivo research. Formulation was robust and easily transfers to scale up. All CQAs and CPPs were within limits, and there is no significant difference found. Stability evaluations, preclinical and clinical pharmacokinetic modeling, and patient usability/acceptability studies are now needed in order to fully exploit the promise of these novel AZN delivery methods.

#### 5. MATERIALS AND METHODS

**5.1. Materials.** AZN was provided as a kind gift sample by Saffron Pharmaceuticals (Faisalabad, Pakistan). Spectrum Medical Industries provided dialysis membranes with a molecular weight cutoff (MWCO) of 12,000–14,000 Da (Houston, TX, USA). Ethanol, polylobate 80, and  $\beta$ -cyclodextrin ( $\beta$ -CD) were obtained from Dae-Jung Chemicals (Seoul, Korea). Chondroitin was procured from E-Merck (Darmstadt, Germany). Throughout the studies, double-distilled water created at an on-site plant was used. The remaining chemicals and solvents were all analytical grade and used just as the supplier had instructed.

**5.2. Preparation of Nanosuspension.** By using the nanoprecipitation approach with a little modification to the previously described procedure, the chondroitin-based nanosuspension was prepared.<sup>32</sup> Chondroitin solution was prepared in 0.66% (v/v) ethanol (10 mL), and pH of the chondroitin solution was raised to 5.5 by adding a solution of NaOH (temperature maintained at 50 °C with 1000 stirring speed). The prepared drug and polymer solution was then injected into 20 mL of distilled water containing 3.5% w/v of Tween 80 and 3.3% w/v of  $\beta$ -CD using a 26-gauge syringe at a steady rate (0.5 mL/min). Using a magnetic stirrer, the mixture was homogenized for 2 h at a continuous agitation speed of 2000 rpm. The final volume of the suspension was collected after an

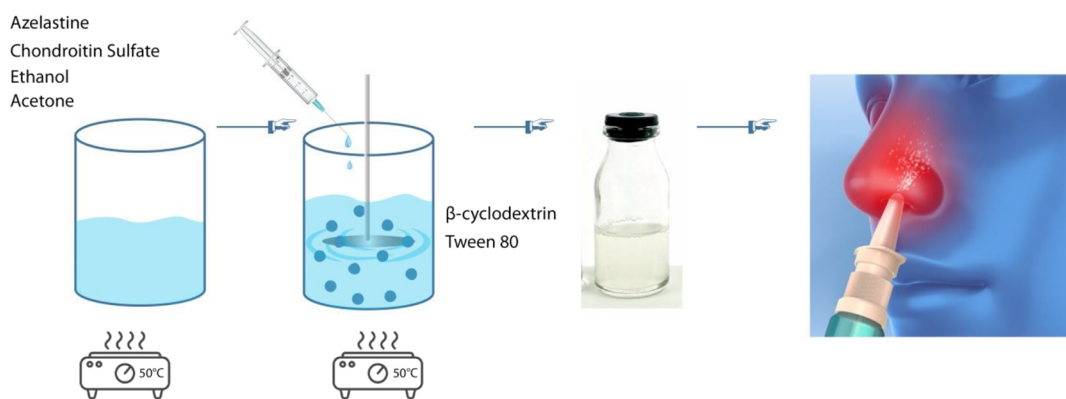


**Figure 13.** Preparation method of the nanosuspension and nano nasal spray.

excess of acetone was evaporated during stirring at a temperature of 50 °C. Using an ultrasonic probe sonicator, the resultant suspension was further sonicated (ZHANYI Sonic, China).

**5.3. Preparation of Nasal Spray Nanoprodukt.** The nasal spray product was prepared by using AZN nanosuspension. Once the nanosuspension was checked for drug entrapment, the required amount of nanosuspension was added into NEOCEL C91 solution. In this preparation, we have used the same excipient as the innovator. Moreover, the prepared nano nasal spray was filled into nasal delivery devices. This project was completed in the Saffron plant, and the plant capabilities of Saffron allow us to support large-scale manufacturing. During lab-scale preparation, we also determined the CQAs and CPPs which were monitored in the scale up (Figure 13).

**5.4. Determination of Entrapment Efficiency.** To generate the NP precipitate, the nano nasal spray was mixed with methanol and centrifuged at 2000 rpm for 30 min. The polymer was precipitated using methanol and settled down. The supernatant was collected and filtered with a 0.4 μm (nylon) filter, and the filtrate was measured for AZN using a laboratory developed high-performance liquid chromatography (HPLC) technique. The Shimadzu LC 20AB HPLC system included a 1000 pump and a UV–vis detector (Tokyo, Japan). The stationary phase was an Agela C18 column (250 × 4.6 mm, 5 μm), while the mobile phase included potassium dihydrogen orthophosphate buffer (pH 7.6) and acetonitrile in the proportions of 50:50 (v/v). The injection volume was 20 μL, the mobile phase flow rate was 1.0 mL/min, and the UV detector was set to a 288 nm wavelength. The acquired chromatograms were compared to the standard, and a triplicate calculation of the drug-loading efficiency was made. The stability and uniformity of the actuator of the nano nasal spray were also determined with the same method (not measured in this project). The entrapment efficiency was determined using eq 1:

$$\begin{aligned} \text{Entrapment efficiency (\%)} \\ &= \frac{\text{Drug added} - \text{Free drug}}{\text{Drug added}} \times 100 \end{aligned} \quad (1)$$

**5.5. Particle Size, PDI, and Zeta Potential.** The mean particle size, PDI, and zeta potential were measured using a particle size analyzer and photon correlation spectroscopy (Zetasizer, Malvern Instruments, UK). This method entailed creating an AZN nanosuspension in filtered water and measuring the PDI and particle diameter right away.<sup>33</sup>

**5.6. FTIR Analysis.** An attenuated total reflection crystal cell-equipped FTIR spectrometer from Thermo Scientific (Nicolet iNS FTIR, USA) was employed in the current experiment. Using a spatula, a little amount of sample was put in the device and then tightly compressed. This technique was used to record the spectra of pure AZN, pure chondroitin, and AZN nanosuspension in the 800–4000 cm<sup>-1</sup> range.<sup>34</sup>

**5.7. Thermal Analysis.** Pure AZN, pure chondroitin, and AZN nanosuspension were submitted to thermal analysis using DSC and TGA techniques. DSC/TGA analysis was performed utilizing a Diamond Series DSC/TGA (Perkin Elmer, St. Louis, MO, USA) instrument with the temperature range of 0–300 °C after loading into a conventional empty aluminum pan. For the blank, identical heating conditions were applied to an empty control pan. Purging nitrogen was used to keep the atmosphere inert with a flow rate of 20 mL/min.

**5.8. PXRD Study.** Pure AZN, pure chondroitin, and AZN nanosuspension were exposed to a PXRD analyzer made by DADVANCE (Bruker, Germany). The instrument was operating at 30 kV and at 15 mA with Cu Kα radiation (1.542 Å) in the range from 5 to 50° diffraction angle (2θ) in steps of 0.02 with a scan step length of 2.00 s. After that, the data were visualized as peak height (intensity) versus 2θ.<sup>35</sup>

**5.9. Morphology Study.** Using SEM (JEOL Ltd., Tokyo, Japan), the morphological analysis was carried out. Raw powder AZN in the crystal form and AZN nanosuspension were all applied to gold-coated dual-sided adhesive tape-coated metal stubs, and SEM images were recorded.

**5.10. In Vitro Release Study.** Pure AZN and nano nasal spray were subjected to in vitro investigations using the dialysis membrane technique. A dialysis bag (MWCO 12,000–14,000 Da) was filled with nano nasal spray containing 1 mg of the drug and dispersed in 5 mL of distilled water. The bag was sealed to form a closed pouch. The dialysis bag was then suspended separately in 500 mL of medium kept at 37 ± 0.5 °C while being continuously stirred at 50 rpm and containing 0.1 N HCl (pH 1.2) and phosphate buffer (pH 7.4). Then, 2.0 mL of samples were taken out at specified intervals up to 8 h and replaced with the same volume from new media under the same circumstances. The resultant filtrate was collected through 0.45 μm pore size and used for HPLC analysis after being diluted in the mobile phase. Using the calibration curve developed during the method validation experiments, the drug concentration in the prepared sample was measured.<sup>36</sup> Percentage release was calculated as reported previously.<sup>37,38</sup>

**5.11. In Vitro Cell Viability Studies.** One of the most crucial markers for biological evaluation for in vitro inves-

tigations is cytotoxicity or cell viability. Different cytotoxicity mechanisms exist for different substances such as medications and pesticides. There are several degradation mechanisms for the cells like cell membrane damage, inhibition of protein synthesis, irreversible binding to receptors, and so forth.<sup>39</sup> We have used this technique to determine the AZN nanosuspension. The human hepatocellular (HepG2) cell line was purchased from the University of Lahore at the American Type Culture Collection (ATCC). Fetal bovine serum (10%) was added to DMEM media (Invitrogen, Thermo-Fisher-Scientific-corporation) to sustain the cells. Streptomycin (50 U/mL, Invitrogen) and penicillin (50 U/mL, Invitrogen) were also added as preservatives. The cells were cultivated and maintained in a 5% CO<sub>2</sub> humidified incubator at 37 °C. Succinate dehydrogenase mitochondrial activity was evaluated using the 3-(4,5-dimethylthiazol-2-yl)-2,5-diphenyltetrazolium bromide (MTT) test a day prior to the nano nasal spray incubation.<sup>40</sup> For 24 h, the cell culture was supplemented with various concentrations of nano nasal spray (50, 100, 150, 200, 400, and 1000 µg/mL). Then, each well received 15 µL of MTT (5 mg/mL) in PBS, which was added after the initial 4 h of incubation at 37 °C. Following careful aspiration of the medium containing MTT, the produced formazan crystals in each well were dissolved in 100 µL of dimethyl sulfoxide, and the absorbance of the resulting solution was then determined at 570 nm using a microplate reader.<sup>41</sup> The cell viability (%) was calculated using eq 2:<sup>35</sup>

$$\% \text{Cell Viability} = \frac{\text{Abs of treated cell} - \text{Abs of blank}}{\text{Abs of Control} - \text{Abs of Blank}} \times 100 \quad (2)$$

**5.12. Hemolytic Investigations.** For the hemolytic test, blood was drawn into a tube containing ethylene diamine tetraacetic acid. AZN nanosuspension with different concentrations (100, 150, and 200 µg) were used. Samples were added into tubes containing blood and held for 24 h and centrifuged at 1500 rpm for 5 min. The supernatant was then collected, and the precipitate was then washed three times with PBS. 200 µL of cleaned blood sediment was received with 3.8 mL of PBS, and the mixture was vortexed for a while. After keeping the samples at 37 °C for 2 h, the mixture was centrifuged at 1600 rpm for 5 min. The absorbance of the supernatant was measured at 541 nm. TX100 was chosen as the positive control in this experiment, and PBS was chosen as the negative control, and hemolysis was calculated using eq 3:

$$\text{Hemolysis\%} = \frac{\text{Abs of sample} - \text{Abs of control}}{\text{Absorbance of lysis} - \text{Abs of control}} \times 100 \quad (3)$$

**5.13. Effects on Expression Levels of Proinflammatory Cytokines.** Proinflammatory cytokine (IL-4), produced basically by Th-2 lymphocytes, trigger strong inflammation in allergic asthma. In the current work, we used mice (30–50 g), which were segregated into four groups. OVA was administered intranasally to challenge the airways after intraperitoneal sensitization to cause allergic asthma. All groups other than the control group received intraperitoneal administration of 20 g of OVA dissolved in aluminum hydroxide solution on days 0 and 14 (2 mg dissolved in 0.1 mL of PBS). All experimental protocols received approval from the RLCP Ethical Review Board (IRB No. RLCP/12/2022), and they were carried out in conformity with the World Medical Association's Declaration of Helsinki.

Control group animals were sham-sensitized as well as challenged with PBS only. Then after 14 days, two groups of mice were given two separate doses of AZN nanosuspension and pure drug suspension according to human dose (137 µg/kg/day). Throughout the treatment period, one group of mice was also given an intranasal challenge with OVA every day. On day 28, all groups were euthanized to isolate total RNA from lung samples. TRIzol method was used to measure the yield and purity of total RNA. Reverse transcription and RNA isolation both employed the same reaction agents and quantities as described in our earlier articles.<sup>42</sup> The cDNA was synthesized and incubated at 42 °C for 60 min and was kept at –20 °C for storage. Utilizing gene-specific primers, amplification by polymerase chain reaction was carried out using the cDNA as a template.

**5.14. Test for Nasal Ciliotoxicity of AZN Nanosuspension.** This investigation was carried out to assess the toxicity of the AZN nanosuspension. To assess the harmful effects of NPs, the goat's nasal mucosa was used. Freshly removed goat nasal mucosa, without the septum, was obtained from the slaughterhouse and treated with a 137 µg/kg/0.5 mL formulation for 6 hours in order to conduct research on nasal ciliotoxicity. The goat weight was 20 kg ± 5, and the dose was adjusted according to human dose, and it was 39.1 µg for 20 kg goat. Before using the animals, ethical committee permission was granted (IRB NO: RLCP/17/2022). The cleaned nasal mucosa was then regularly processed with 10% buffered formalin. Hematoxylin and eosin was used to stain the sections that were cut on glass slides. To look for tissue damage, mucosa was examined under a light microscope. Negative control treated with PBS and positive control treated with ethanol were used for comparison.

**5.15. Postpreparation Test.** **5.15.1. Microbiological Studies.** The biological activity of nano nasal spray against germs (*Pseudomonas aeruginosa* and *Staphylococcus aureus*) was determined by microbiological investigations. The test microbe (0.2 mL) was seeded onto a layer of nutrient agar (20 mL), which was then allowed to set up in the Petri dish. A sterile borer with a 4 mm diameter was used to create cups on the hardened agar layer. After that, each cup was filled with a volume of the nasal spray each of which contained an equal amount of the drug. The Petri plates were incubated at 32 °C for 72 h after being kept in incubator. After the completion of time, CFUs were calculated on each plate. Three copies of the observation and measurements were made.<sup>43</sup>

**5.15.2. Physical Appearance, Viscosity, and pH Measurement.** The physical characteristics of the nano nasal spray were examined. After that, 1% dispersion made in aqueous medium had its pH measured using a digital pH meter (Ino lab WTW 730, USA). The viscosities of the developed nano nasal spray were assessed using a Brookfield viscometer (Model DV-II, Spindle #21) at 0.5, 1, and 2 rpm.

**5.15.3. In Vitro Diffusion Studies.** In order to study the diffusion of nano nasal spray, Franz diffusion cell was employed. Silicon membrane was used in this experiment. The penetration of the nano nasal spray was evaluated using a vertical Franz diffusion cell (SES Analytical Systems, GmbH, Germany) with a donor surface area of 1.2 cm<sup>2</sup> and a receptor volume of 5.2 mL with the silicon membrane. A semisynthetic silicon SAMCO membrane (Nuneaton, UK) divided the donor and receptor chambers of the Franz diffusion cell. A sample of the nano nasal spray was placed within the 1.0 mL volume. PBS (7.4 pH) was circulating in the receptor chamber with a maintained

temperature of 37 °C. The membrane and receptor phase were in contact for an hour at a temperature of  $37 \pm 0.5$  °C before the experiment. Samples (0.5 mL) were obtained at specified intervals throughout the receptor phase's 8 h (0.5, 1, 2, 4, 6, and 8 h) and assessed by HPLC at 288 nm, while the cell was replenished with an equivalent quantity of freshly made PBS.<sup>35,44–46</sup>

**5.15.4. Nanosuspension Dosage Forms: Process Variable and Scale Up.** Drug nanosuspensions can be made using a top-down, bottom-up, or hybrid approach. The initial focus of the development process for nanosuspension formulations should be on screening to find the lead formulation that produces stable nanosuspensions with the necessary therapeutic effectiveness and pharmacokinetic features in both animals and people. After that, the scale up procedure should be adjusted to identify the crucial process parameters. Liquid dispersion of solid drugs, like nanosuspensions, are NPs that have a surfactant or a polymer stabilizing them.<sup>47</sup> It has been demonstrated that nanosizing is a useful technique for a “brick dust candidate” an active minority. When included in medication formulations, NPs can offer numerous pharmacokinetic, efficacy, safety, and targeting advantages. Several nanodrugs have been approved by FDA, and some carrier system was included in USP pharmacopeia. Even more nanodrugs are being tested in clinical studies for a wide range of diseases, and many have already reached clinical use. The biomedical<sup>48</sup> and pharmaceutical sciences are combined with nanotechnology in the relatively new and fast developing discipline of nanomedicine. Scale up of pharmaceuticals products always remain a challenge, and a lot of products have got several issues during technology transfer. A nanosuspension's stability and toughness are primarily numerous formulation and process factors are in control. Choosing the best steric and electrostatic stabilizer is essential. When creating a nanosuspension, quantity is crucial. In this article, we also emphasize on process variables influencing the scale up. After optimization of formulation and completion on lab scale, our aim was to transfer it to production department for scale up. We have identified the process variables and quality material attributes which can significantly impact the scale up. All critical parameters and their solution to avoid failure of the product are summarized in this work.

**5.16. Analytical Statistics.** One-way ANOVA and Tukey's test were used in the statistical analysis, which was done using the Graph-Pad Prism (v.5, San Diego, CA, USA) software. The in vitro parameters are presented as mean  $\pm$  SD of three independent experiments. The in vivo parameters are presented as mean  $\pm$  SD of six independent experiments. Statistical significance is defined as a *p* value of 0.05.

## AUTHOR INFORMATION

### Corresponding Author

**Yasir Mehmood** – Department of Pharmaceutics, Faculty of Pharmaceutical Sciences, Government College University Faisalabad, Faisalabad 38040, Pakistan; Riphah Institute of Pharmaceutical Sciences (RIPS), Riphah International University, Faisalabad, Punjab 44000, Pakistan;  
● [orcid.org/0000-0002-7786-2755](https://orcid.org/0000-0002-7786-2755);  
Email: [Yasirmehmoodamjad@gmail.com](mailto:Yasirmehmoodamjad@gmail.com)

### Authors

**Hira Shahid** – Department of Pharmacology, Faculty of Pharmaceutical Sciences, Government College University Faisalabad, Faisalabad 38040, Pakistan

**Muhammad Abbas** – Imran Adress College of Pharmacy, Sialkot 51310, Pakistan

**Umar Farooq** – Faculty of Pharmacy, Grand Asian University, Sialkot 51040 Punjab, Pakistan

**Sultan Alshehri** – Department of Pharmaceutics, College of Pharmacy, King Saud University, Riyadh 11451, Saudi Arabia; ● [orcid.org/0000-0002-0922-9819](https://orcid.org/0000-0002-0922-9819)

**Prawez Alam** – Department of Pharmacognosy, College of Pharmacy, Prince Sattam Bin Abdul Aziz University, Al-Kharj 11942, Saudi Arabia; ● [orcid.org/0000-0002-7632-3426](https://orcid.org/0000-0002-7632-3426)

**Faiyaz Shakeel** – Department of Pharmaceutics, College of Pharmacy, King Saud University, Riyadh 11451, Saudi Arabia; ● [orcid.org/0000-0002-6109-0885](https://orcid.org/0000-0002-6109-0885)

**Mohammed M. Ghoneim** – Department of Pharmacy Practice, College of Pharmacy, AlMaarefa University, Ad Diriyah 13713, Saudi Arabia

Complete contact information is available at:

<https://pubs.acs.org/10.1021/acsomega.3c02186>

## Notes

The authors declare no competing financial interest.

## ACKNOWLEDGMENTS

“The authors are thankful to the Researchers Supporting Project (number RSP2023R146) at King Saud University, Riyadh, Saudi Arabia for supporting this research.” “The authors are also thankful to the Prince Sattam bin Abdulaziz University for supporting this work via project number (PSAU/2023/R/1444).” “The authors are also grateful to the AlMaarefa University for their generous support.”

## REFERENCES

- (1) Hsu, J.; Peters, A. T. Pathophysiology of chronic rhinosinusitis with nasal polyp. *Am. J. Rhinol. Allergy* **2011**, *25*, 285–290.
- (2) Lee, S.; Lane, A. P. Chronic rhinosinusitis as a multifactorial inflammatory disorder. *Curr. Infect. Dis. Rep.* **2011**, *13*, 159–168.
- (3) Lee, C.; Corren, J. Review of azelastine nasal spray in the treatment of allergic and non-allergic rhinitis. *Expert Opin. Pharmacother.* **2007**, *8*, 701–709.
- (4) Ratner, P. H.; Hampel, F.; Bavel, J. V.; Amar, N. J.; Daftary, P.; Wheeler, W.; Sacks, H. Combination therapy with azelastine hydrochloride nasal spray and fluticasone propionate nasal spray in the treatment of patients with seasonal allergic rhinitis. *Ann. Allergy Asthma Immunol.* **2008**, *100*, 74–81.
- (5) Lumry, W. R. A review of the preclinical and clinical data of newer intranasal steroids used in the treatment of allergic rhinitis. *J. Allergy Clin. Immunol.* **1999**, *104*, S150–S159.
- (6) Greiner, A. N.; Hellings, P. W.; Rotiroti, G.; Scadding, G. K. Allergic rhinitis. *Lancet* **2011**, *378*, 2112–2122.
- (7) Baena-Cagnani, C. E. Safety and tolerability of treatments for allergic rhinitis in children. *Drug Saf.* **2004**, *27*, 883–898.
- (8) Karaki, M.; Akiyama, K.; Mori, N. Efficacy of intranasal steroid spray (mometasone furoate) on treatment of patients with seasonal allergic rhinitis: comparison with oral corticosteroids. *Auris Nasus Larynx* **2013**, *40*, 277–281.
- (9) Ito, H.; Nakamura, Y.; Takagi, S.; Sakai, K. Effects of azelastine on the level of serum interleukin-4 and soluble CD23 antigen in the treatment of nasal allergy. *Arzneim. Forsch.* **1998**, *48*, 1143–1147.
- (10) Savale, S. K. UV spectrophotometric method development and validation for quantitative estimation of azelastine HCl. *Asian J. Res. Chem. Pharm. Sci.* **2017**, *5*, 83–86.
- (11) Alshehri, S.; Shakeel, F. Solubility determination, various solubility parameters and solution thermodynamics of sunitinib malate in some cosolvents, water and various (Transcutol + water) mixtures. *J. Mol. Liq.* **2020**, *307*, No. 112970.

- (12) Da Silva, F. L. O.; Marques, M. B. D. F.; Kato, K. C.; Carneiro, G. Nanonization techniques to overcome poor water-solubility with drugs. *Expert Opin. Drug Discovery* **2020**, *15*, 853–864.
- (13) Alanazi, A.; Alshehri, S.; Altamimi, M.; Shakeel, F. Solubility determination and three dimensional Hansen solubility parameters of gefitinib in different organic solvents: Experimental and computational approaches. *J. Mol. Liq.* **2020**, *299*, 11211.
- (14) Kalam, M. A.; Alshamsan, A.; Alkholief, M.; Alsarra, I. A.; Ali, R.; Haq, N.; Anwer, M. K.; Shakeel, F. Solubility measurement and various solubility parameters of glipizide in different neat solvents. *ACS Omega* **2020**, *5*, 1708–1716.
- (15) Bhakay, A.; Rahman, M.; Dave, R. N.; Bilgili, E. Bioavailability enhancement of poorly water-soluble drugs via nanocomposites: Formulation—Processing aspects and challenges. *Pharmaceutics* **2018**, *10*, 86.
- (16) Shakeel, F.; Alshehri, S.; Ibrahim, M. A.; Altamimi, M.; Haq, N.; Elzayat, E. M.; Shazly, G. A. Solubilization and thermodynamic properties of simvastatin in various micellar solution of different non-ionic surfactants: Computational modeling and solubilization capacity. *PLoS One* **2021**, *16*, No. 0249485.
- (17) Alshehri, S.; Imam, S. S.; Hussain, A.; Altamimi, M. A.; Alruwaili, N. K.; Aloatibi, F.; Alanazi, A.; Shakeel, F. Potential of solid dispersions to enhance solubility, bioavailability, and therapeutic efficacy of poorly water-soluble drugs: newer formulation techniques, current marketed scenario and patents. *Drug Delivery* **2020**, *27*, 1625–1643.
- (18) Tran, P.; Pyo, Y.-C.; Kim, D.-H.; Lee, S.-E.; Kim, J.-K.; Park, J.-S. Overview of the manufacturing methods of solid dispersion technology for improving the solubility of poorly water-soluble drugs and application to anticancer drugs. *Pharmaceutics* **2019**, *11*, 132.
- (19) Haimhoffer, Á.; Ruzsnyak, A.; Reti-Nagy, K.; Vasvari, G.; Varadi, J.; Vecsernyes, M.; Bacskay, I.; Feher, P.; Ujhelyi, Z.; Fenyvesi, F. Cyclodextrins in drug delivery systems and their effects on biological barriers. *Sci. Pharm.* **2019**, *87*, 33.
- (20) Ahlawat, J.; Henriquez, G.; Narayan, M. Enhancing the delivery of chemotherapeutics: role of biodegradable polymeric nanoparticles. *Molecules* **2018**, *23*, 2157.
- (21) Sahoo, S. K.; Dilnawaz, F.; Krishnakumar, S. Nanotechnology in ocular drug delivery. *Drug Discovery Today* **2008**, *13*, 144–151.
- (22) Arshad, M. S.; Zafar, S.; Yousef, B.; Alyassin, Y.; Ali, R.; AlAsiri, A.; Chang, M.-W.; Ahmad, Z.; Elkordy, A. A.; Faheem, A.; et al. A review of emerging technologies enabling improved solid oral dosage form manufacturing and processing. *Adv. Drug Delivery Rev.* **2021**, *178*, No. 113840.
- (23) Far, J.; Abdel-Haq, M.; Gruber, M.; Ammar, A. A. Developing biodegradable nanoparticles loaded with mometasone furoate for potential nasal drug delivery. *ACS Omega* **2020**, *5*, 7432–7439.
- (24) Muxika, A.; Etxabide, A.; Uranga, J.; Guerrero, P.; de la Caba, K. Chitosan as a bioactive polymer: Processing, properties and applications. *Int. J. Biol. Macromol.* **2017**, *105*, 1358–1368.
- (25) Jacob, S.; Nair, A. B.; Shah, J. Emerging role of nanosuspensions in drug delivery systems. *Biomater. Res.* **2020**, *24*, 3.
- (26) Tiwari, A.; Mishra, M. K.; Shukla, A.; Yadav, S. K. Microsponge: An augmented drug delivery system. *Am. J. PharmTech. Res.* **2016**, *6*, 79–95.
- (27) Adriaensens, G.F.; Lim, K.H.; Fokkens, W.J. Safety and efficacy of a bioabsorbable fluticasone propionate-eluting sinus dressing in postoperative management of endoscopic sinus surgery: a randomized clinical trial. In *International forum of allergy & rhinology*; Wiley Online Library, 2017.
- (28) Ballal, N. V.; Kundabala, M.; Bhat, K. S.; Acharya, S.; Ballal, M.; Kumar, R.; Prakash, P. Y. Susceptibility of *Candida albicans* and *Enterococcus faecalis* to chitosan, chlorhexidine gluconate and their combination in vitro. *Aust. Endod. J.* **2009**, *35*, 29–33.
- (29) Marple, B. F.; Stankiewicz, J. A.; Baroody, F. M.; Chow, J. M.; Conley, D. B.; Corey, J. P.; Ferguson, B. J.; Kern, R. C.; Lusk, R. P.; Naclerio, R. M.; Orlandi, R. R.; Parker, M. J. Diagnosis and management of chronic rhinosinusitis in adults. *Postgrad. Med.* **2009**, *121*, 121–139.
- (30) Bonifacio, B. V.; da Silva, P. B.; Ramos, M. A. D. S.; Negri, K. M. S.; Bauab, T. M.; Chorilli, M. Nanotechnology-based drug delivery systems and herbal medicines: a review. *Int. J. Nanomed.* **2014**, *9*, 1–15.
- (31) Kumar, S.; Dilbaghi, N.; Saharan, R.; Bhanjana, G. Nanotechnology as emerging tool for enhancing solubility of poorly water-soluble drugs. *BioNanoScience* **2012**, *2*, 227–250.
- (32) Perween, N.; Alshehri, S.; Easwari, T. S.; Verma, V.; Faiyazuddin, M.; Alanazi, A.; Shakeel, F. Investigating the feasibility of mefenamic acid nanosuspension for pediatric delivery: Preparation, characterization, and role of excipient. *Processes* **2021**, *9*, 574.
- (33) Mehmood, Y.; Khan, I. U.; Shahzad, Y.; Khan, R. U.; Iqbal, M. S.; Khan, H. A.; Khalid, I.; Yusaf, A. M.; Khalid, S. H.; Asghar, S.; et al. In-vitro and in-vivo evaluation of velpatasvir-loaded mesoporous silica scaffolds. A prospective carrier for drug bioavailability enhancement. *Pharmaceutics* **2020**, *12*, 307.
- (34) Mehmood, Y.; Khan, I. U.; Shahzad, Y.; Khan, R. U.; Khalid, S. H.; Yusaf, A. M.; Hussain, T.; Asghar, S.; Khalid, I.; Asif, M.; Shah, S. U. Amino-decorated mesoporous silica nanoparticles for controlled sofosbuvir delivery. *Eur. J. Pharm. Sci.* **2020**, *143*, No. 105184.
- (35) Mehmood, Y.; Khan, I. U.; Shahzad, Y.; Khalid, S. H.; Asghar, S.; Irfan, M.; Asif, M.; Khalid, I.; Yusaf, A. M.; Hussain, T. Facile synthesis of mesoporous silica nanoparticles using modified sol-gel method: Optimization and in vitro cytotoxicity studies. *Pak. J. Pharm. Sci.* **2019**, *32*, 1805–1812.
- (36) Zhang, Y.; Huo, M.; Zhou, J.; Zou, A.; Li, W.; Yao, C.; Xie, S. DDSolver: an add-in program for modeling and comparison of drug dissolution profiles. *AAPS J.* **2010**, *12*, 263–271.
- (37) Barkat, K.; Ahmad, M.; Minhas, M. U.; Khalid, I.; Nasir, B. Development and characterization of pH-responsive polyethylene glycol-co-poly (methacrylic acid) polymeric network system for colon target delivery of oxaliplatin: Its acute oral toxicity study. *Adv. Polym. Technol.* **2018**, *37*, 1806–1822.
- (38) Khalid, I.; Ahmad, M.; Minhas, M. U.; Barkat, K. Preparation and characterization of alginate-PVA-based semi-IPN: controlled release pH-responsive composites. *Polym. Bull.* **2018**, *75*, 1075–1099.
- (39) Aslantürk, Ö. S. In vitro cytotoxicity and cell viability assays: principles, advantages, and disadvantages. In *Genotoxicity-A predictable risk to our actual world*; 2018; Vol. 2, pp 64–80.
- (40) Mosmann, T. Rapid colorimetric assay for cellular growth and survival: application to proliferation and cytotoxicity assays. *J. Immunol. Methods* **1983**, *65*, 55–63.
- (41) Patel, S.; Gheewala, N.; Suthar, A.; Shah, A. In-vitro cytotoxicity activity of Solanum nigrum extract against HeLa cell line and Vero cell line. *Int. J. Pharm. Pharm. Sci.* **2009**, *1*, 38–46.
- (42) Shahid, H.; Shahzad, M.; Shabbir, A.; Saghir, G. Immunomodulatory and anti-inflammatory potential of curcumin for the treatment of allergic asthma: effects on expression levels of pro-inflammatory cytokines and aquaporins. *Inflammation* **2019**, *42*, 2037–2047.
- (43) Baek, J. H.; Lee, S.-Y.; Oh, S.-W. Enhancing safety and quality of shrimp by nanoparticles of sodium alginate-based edible coating containing grapefruit seed extract. *Int. J. Biol. Macromol.* **2021**, *189*, 84–90.
- (44) Thakur, S.; Singh, H.; Singh, A.; Kaur, S.; Sharma, A.; Singh, S. K.; Kaur, S.; Kaur, G.; Jain, S. K. Thermosensitive injectable hydrogel containing carboplatin loaded nanoparticles: A dual approach for sustained and localized delivery with improved safety and therapeutic efficacy. *J. Drug Delivery Sci. Technol.* **2020**, *58*, No. 101817.
- (45) Abdul, A. H.; Bala, A. G.; Chintaginjala, H.; Manchikanti, S. P.; Kamsali, A. K.; Dasari, R. R. D. Equator assessment of nanoparticles using the design-expert software. *Int. J. Pharm. Sci. Nanotechnol.* **2020**, *13*, 4766–4772.
- (46) Singare, D. S.; Marella, S.; Gowthamarajan, K.; Kulkarni, G. T.; Vooturi, R.; Rao, P. S. Optimization of formulation and process variable of nanosuspension: An industrial perspective. *Int. J. Pharm.* **2010**, *402*, 213–220.
- (47) Ventola, C. L. Progress in nanomedicine: approved and investigational nanodrugs. *Pharm. Ther.* **2017**, *42*, 742–755.

(48) Phadtare, D. G.; Gaika, M. N.; Aher, S. S. Formulation and characterization of nanoemulsion based nasal spray of azelastine hydrochloride. *Res. J. Top. Cosmet. Sci.* **2016**, *7*, 55–66.